Supplemental material

Tuncel et al., https://doi.org/10.1084/jem.20182002

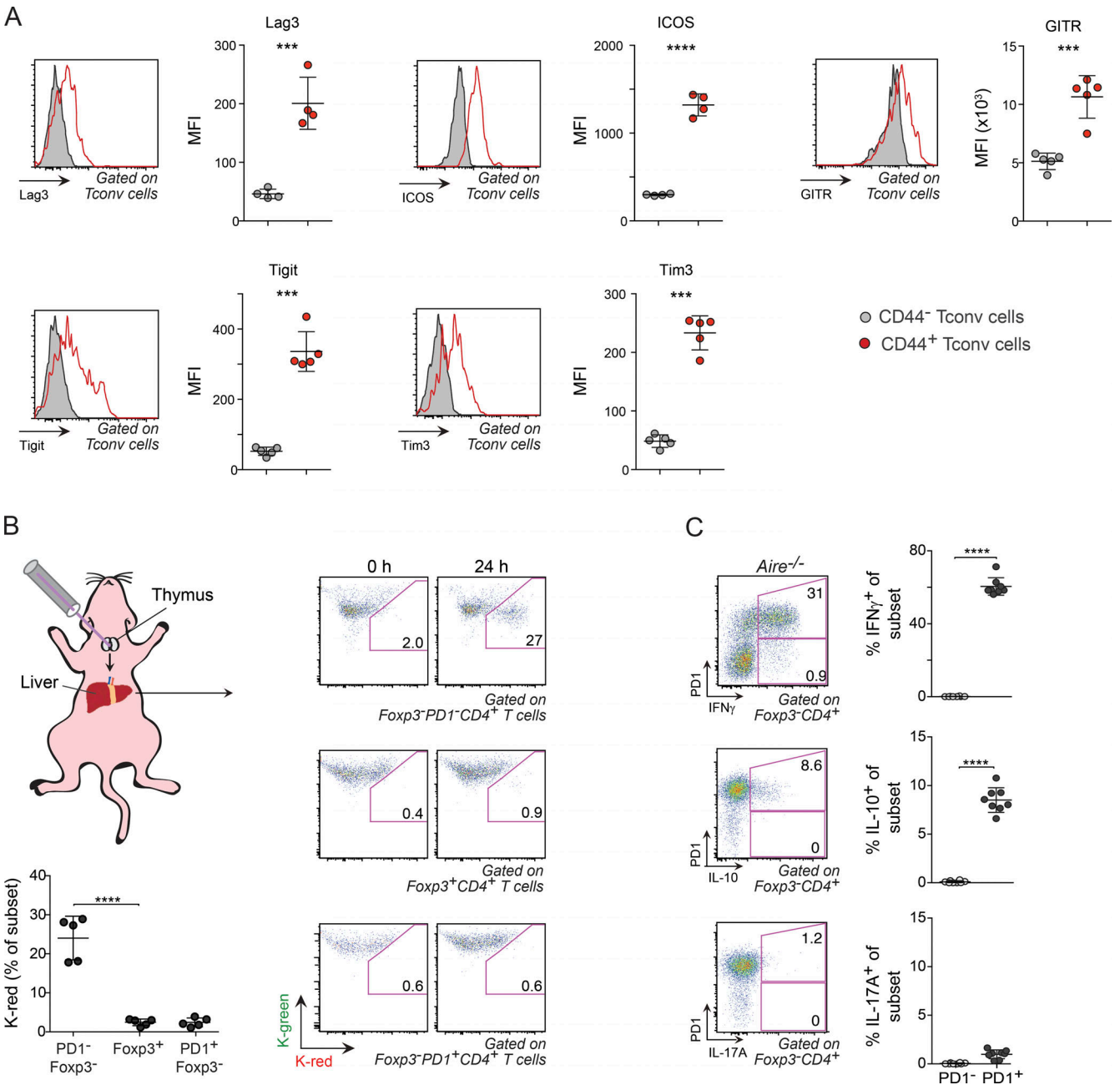

Figure S1. **Phenotype and origin of effector T cells in liver of *Aire*$^{-/-}$ perinates. (A)** Expression of signaling and costimulatory receptors on perinatal liver CD44$^+$ T conv cells. Representative histograms and summarizing mean fluorescence intensity (MFI) data from flow cytometric analyses of liver T conv cells from 12-d-old *Aire*$^{-/-}$ mice (n = 4 mice/group). **(B)** Naive T conv cells constituted the majority of newly exported CD4$^+$ thymocytes in the liver of 5-d-old mice. Thymocytes were tagged in 4-d-old *Kaede*/B6.*Aire*$^{-/-}$ mice through light exposure. 24 h later, the proportion of tagged (photoconverted) CD4$^+$ T cells was determined in the liver. Right: Pseudocolor plots show representative examples of photoconverted naive (PD-1$^-$) T conv cells, Foxp3$^+$ cells, and PD-1$^+$ T conv cells. Bottom: Summary of frequency data (n = 5 mice/group). **(C)** Cytokine production by PD-1$^+$ and PD-1$^-$ liver T conv cells. Flow-cytometric pseudocolor plots and summary data of IFNγ–, IL-10–, and IL-17A–producing T conv cells from the liver of 8-d-old *Aire*$^{-/-}$ mice (n = 8 mice/group). Data are pooled from at least two independent experiments. Data are shown as mean ± SD. ***, P ≤ 0.001; ****, P ≤ 0.0001 (Student's t test).

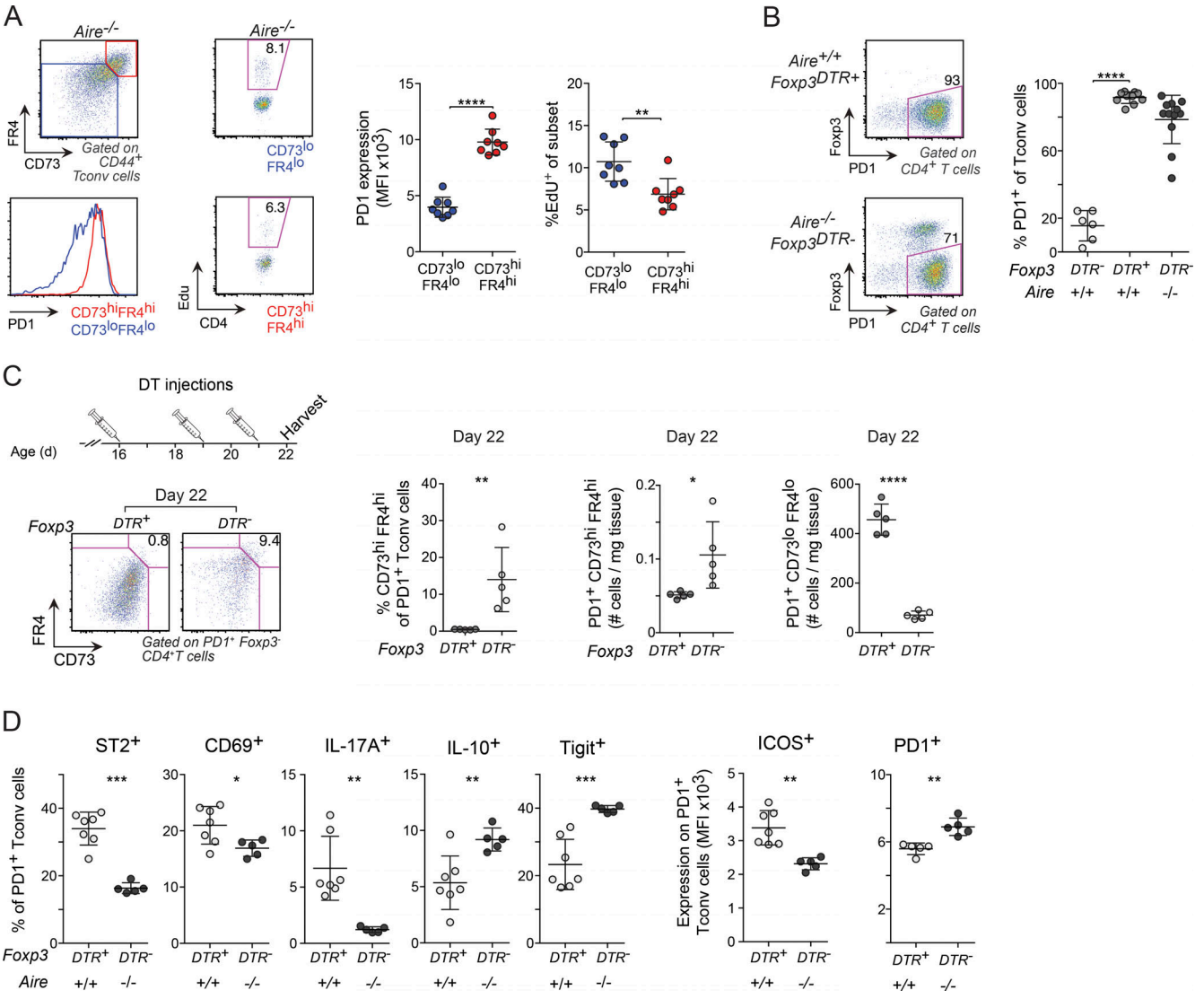

Figure S2. **Phenotypes of effector and anergic cells in *Aire*$^{-/-}$ and T reg cell–depleted perinates. (A)** Upper left: Gating strategy of anergic (red) and effector (blue) CD44$^+$ T conv cells from the liver of 10-d-old *Aire*$^{-/-}$ mice. Lower left: Representative histogram of PD-1 expression. Center left: Representative flow-cytometric plots with gates depicting proliferating (EdU$^+$) effector (top) and anergic (bottom) cells in liver from 12-d-old *Aire*$^{-/-}$ mice, analyzed 4 h after EdU injection. Center and far right: Summary of PD-1 mean fluorescence intensity (MFI) and percentage EdU$^+$ cells (n = 8 mice/group). **(B)** Frequency of PD-1$^+$ T conv cells in the liver of 10-d-old *Foxp3*$^{DTR+}$ and *Foxp3*$^{DTR-}$ perinates after treatment with DT on days 3, 5, and 7 after birth. Left: Representative flow-cytometric plots of CD4$^+$ T cells. Right: Summary of percentage PD-1 (n = 6–12 mice/group). **(C)** Frequency and number of anergic and effector cells in T reg cell–depleted perinates. Upper left: Treatment regimen for DT injection. Bottom left and right: Representative flow-cytometric plots and summary data (n = 5 mice/group). **(D)** PD-1$^+$ T conv cells in T reg cell–depleted perinates were phenotypically distinct from PD-1$^+$ T conv cells in *Aire*$^{-/-}$ mice. Frequencies of cytokine- (after stimulation with phorbol myristate acetate and ionomycin) and cell surface–expressing liver PD-1$^+$ T conv cells of 10-d-old *Aire*$^{+/+}$*Foxp3*$^{DTR+}$ and *Aire*$^{-/-}$ *Foxp3*$^{DTR-}$ mice (treated with DT as in B) as determined by flow cytometry (n = 5–7 mice/group). Data are pooled from at least two independent experiments and show mean ± SD. Statistical analyses as in Fig. S1. *, P ≤ 0.05; **, P ≤ 0.01; ***, P ≤ 0.001; ****, P ≤ 0.0001.

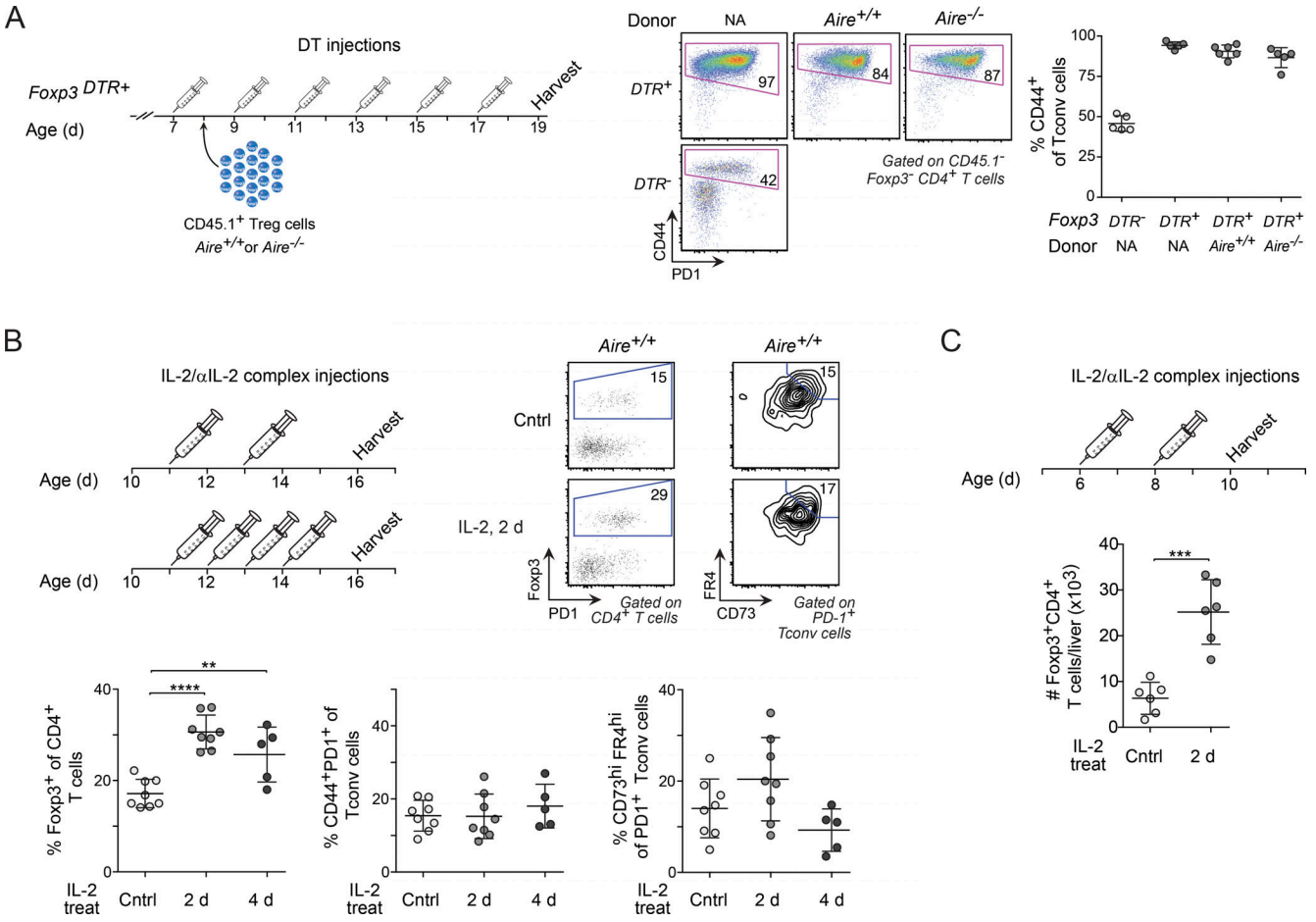

Figure S3. **Impact of T reg cells on effector cell differentiation and the abundance of anergic cells in the perinatal liver. (A)** Frequency of CD44$^+$ T conv cells. Left: Regimen for adoptive T reg cell–transfer and DT treatment. Right: Representative flow-cytometric plots and summary data (n = 5–6 mice/group). **(B)** Treatment with IL-2 increased the number of T reg cells in the liver without affecting the proportion of anergic cells. *Aire*$^{+/+}$ mice were treated with low doses of IL-2/anti–IL-2 mAb complexes daily or every second day between days 11 and 14 after birth, after which the proportions of various CD4$^+$ T cell subsets (as indicated) were determined on day 16. Upper left: Treatment regimen. Upper right: Representative flow-cytometric dot and contour plots of total CD4$^+$ T cells and PD-1$^+$ T conv cells in treated and control (vehicle alone) mice. Bottom: Summary data for percentages of T reg cells, CD44$^+$PD-1$^+$ T conv cells, and anergic cells (n = 5–8 mice/group). **(C)** Number of T reg cells in 10-d-old *Aire*$^{+/+}$ mice after two injections of IL-2/anti–IL-2 mAb complexes on days 6 and 8 after birth (using the same dose of cytokine/antibodies as in B; n = 6 mice/group). Data are pooled from at least two independent experiments and show mean ± SD. Statistical analyses as in Fig. S1. **, P ≤ 0.01; ***, P ≤ 0.001; ****, P ≤ 0.0001.

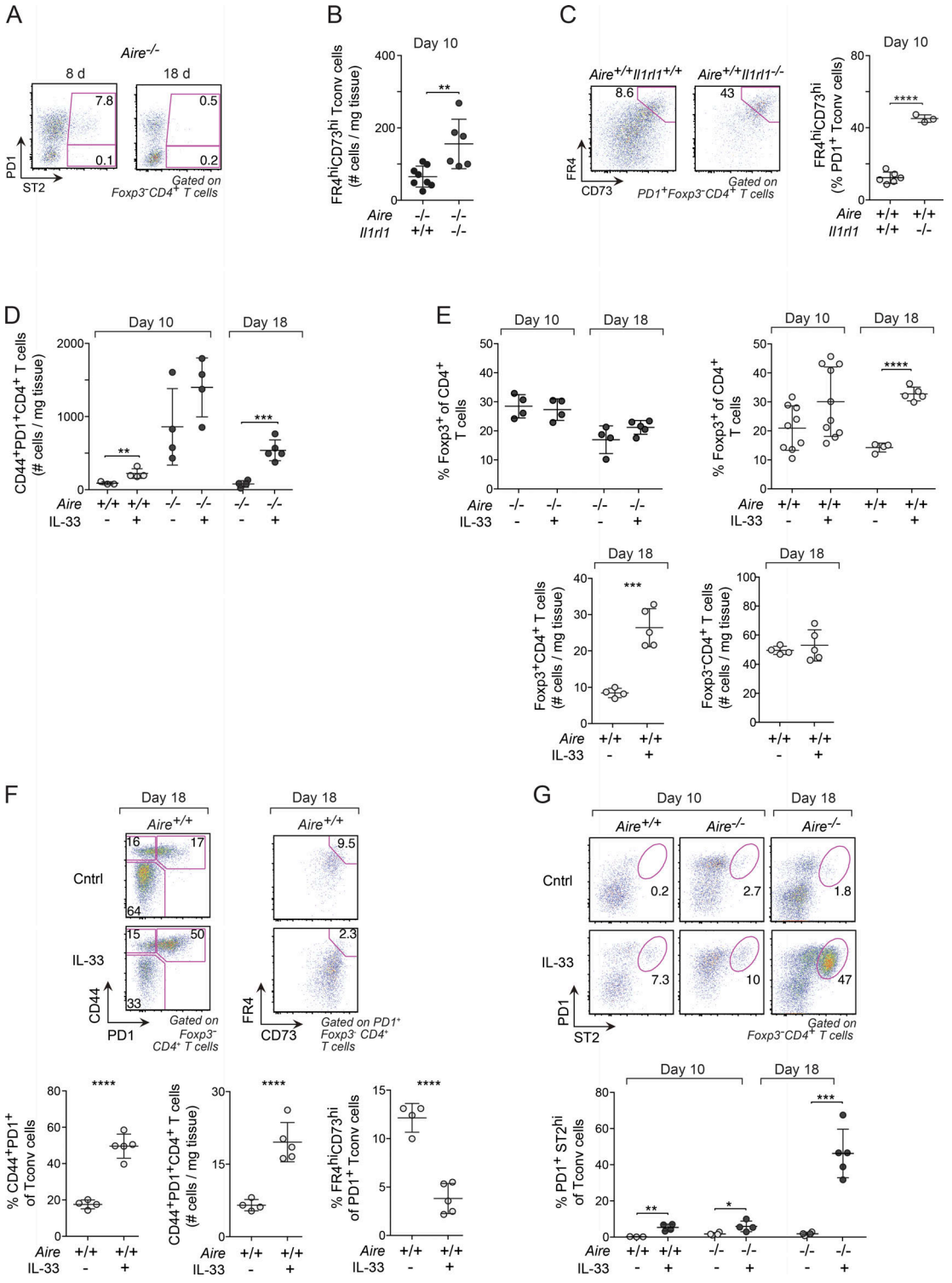

Figure S4. **IL-33 inhibited anergy but promoted T reg cell proliferation and ST2 expression by liver T conv cells. (A)** Representative flow-cytometric plots of T conv cells from 8–18-d-old *Aire*$^{-/-}$ mice (see Fig. 7 A for summary data of ST2^{+}PD-1^{+} and ST2^{+}PD-1^{-} frequencies). **(B and C)** Impact of ST2 deficiency on the number (n = 6–8 mice/group; B) and frequency (n = 3–6 mice/group; C) of anergic cells in 10-d-old *Aire*$^{-/-}$ (B) and *Aire*$^{+/+}$ mice (C). **(D)** Number of CD44^{+}PD-1^{+} T conv cells after treatment with rIL-33 (see Fig. 7 E for treatment regimen). Days 10 and 18, as indicated on top of the scatter plots, represent the days of harvest (n = 4–5 mice/group). **(E)** Frequency and number of liver T reg cells in mice treated with rIL-33. Top: Frequency of T reg cells in *Aire*$^{-/-}$ (left) and *Aire*$^{+/+}$ (right) mice (treated with rIL-33 as in Fig. 7 E). Bottom: Number of T reg cells (left) and T conv (right) cells in *Aire*$^{+/+}$ mice treated with rIL-33 (n = 4–10 mice/group). **(F)** Impact of rIL-33 treatment on total and anergic liver CD44^{+}PD-1^{+} T conv cells in 18-d-old *Aire*$^{+/+}$ mice (n = 4–5 mice/group; see Fig. 7 E for treatment regimen). **(G)** Frequency of ST2^{+} T conv cells in mice treated with rIL-33. Top: Representative flow-cytometric plots. Bottom: Summary data (n = 3–5 mice/group). Data are pooled from at least two independent experiments and show mean ± SD. Statistical analyses as in Fig. S1. **, P ≤ 0.01; ***, P ≤ 0.001; ****, P ≤ 0.0001.

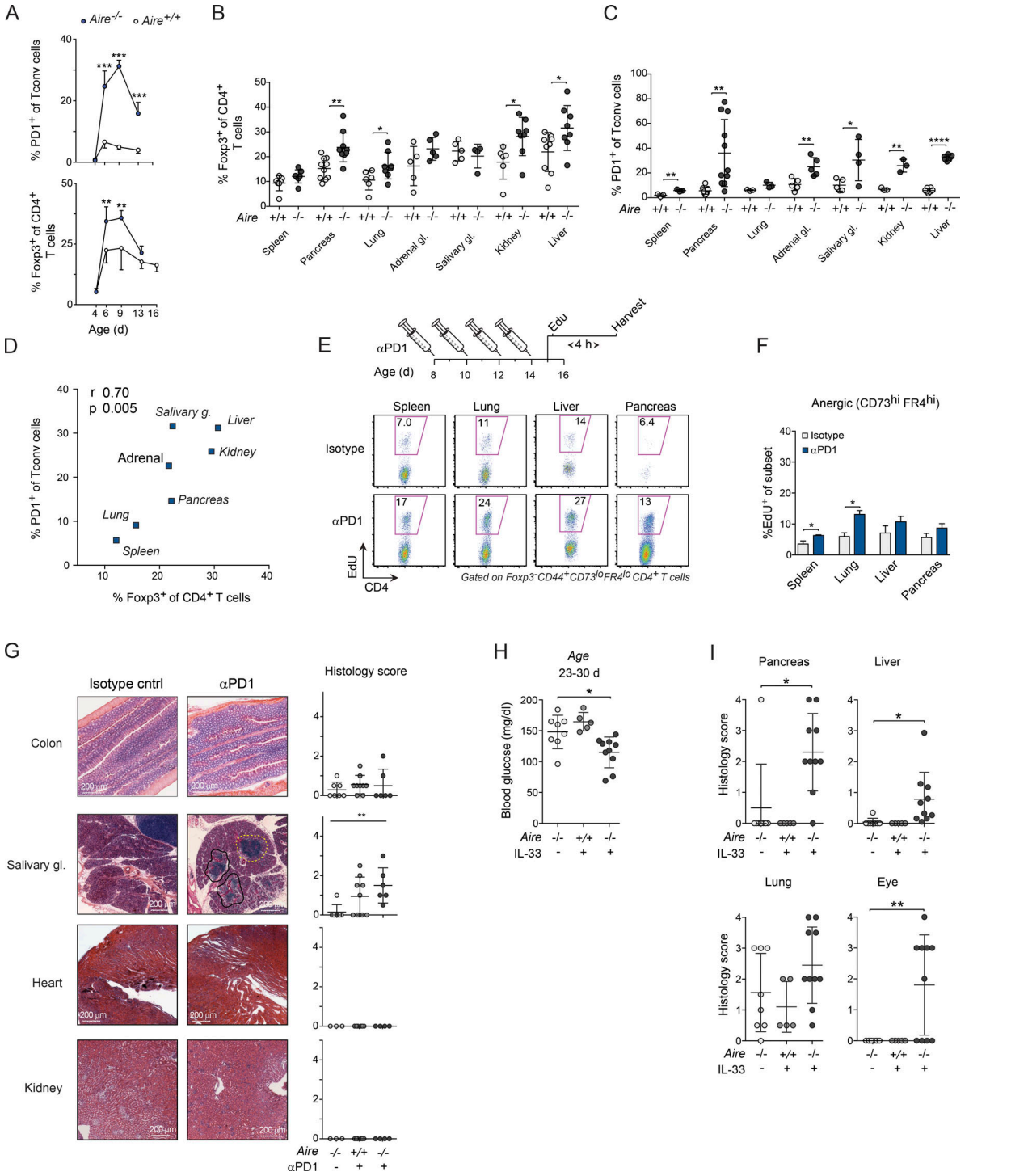

Figure S5. **Impact of inhibiting PD-1 or stimulating ST2 signaling on T cell proliferation and autoimmunity in NOD perinates. (A–D)** PD-1+ T conv cells were enriched in several nonlymphoid organs of NOD.*Aire*$^{-/-}$ perinates. **(A)** Frequencies of PD-1+ Tc onv cells (top) and T reg cells (bottom; gated as in Figs. 1 C and 2 A, respectively) from liver of NOD.*Aire*$^{-/-}$ and *Aire*$^{+/+}$ littermates of various ages (n = 4–9 mice/group). **(B and C)** Proportions of T reg (B) and PD-1+ T conv (C) cells in the spleen and nonlymphoid organs of 8–10-d-old NOD.*Aire*$^{-/-}$ and *Aire*$^{+/+}$ littermates (n = 3–11 mice/group). **(D)** Correlation between frequencies of T reg cells (x axis) and PD-1+ T conv cells (y axis) in the spleen and nonlymphoid organs of 8–10-d-old NOD.*Aire*$^{-/-}$ mice (median values of data shown in B and C; n = 3–9 mice/group). **(E)** Proliferation of CD44+CD73loFR4lo T conv cells from various organs of 15-d-old NOD.*Aire*$^{-/-}$ mice treated with an αPD-1 blocking mAb (or an isotype-matched control mAb) between days 8 and 14 after birth. Cells were analyzed 4 h after EdU injection (data are summarized in Fig. 9 A). **(F)** Corresponding summary data (as in Fig. 9 A) for cells with an anergic phenotype (gated as in Fig. 5 A; n = 3–6 mice/group). **(G)** Data from the same experiment as that depicted in Fig. 9, C and D (n = 6–9 mice/group). Scale bars, 200 µm. **(H)** Blood-glucose levels in NOD.*Aire*$^{-/-}$ mice treated with rIL-33 as compared with controls (vehicle treated; n = 5–10 mice/group). **(I)** Histological scores related to data depicted in Fig. 9 E (n = 5–10 mice/group). Data are pooled from at least two independent experiments and show mean ± SD. Statistical analyses as in Fig. S1. *, P ≤ 0.05; **, P ≤ 0.01; ***, P ≤ 0.001; ****, P ≤ 0.0001.